ORIGINAL ARTICLE

Patient-derived organoids of bladder cancer recapitulate antigen expression profiles and serve as a personal evaluation model for CAR-T cells *in vitro*

Lei Yu[1,2,3†] (iD), Zhichao Li[1,2,3†], Hongbin Mei[1†], Wujiao Li[1,2,3], Dong Chen[1], Lisa Liu[1], Zhongfu Zhang[1], Yangyang Sun[1,2,3], Fei Song[1,2,3], Wei Chen[1,2,3,4] & Weiren Huang[1,2,3,4,5]

[1]Shenzhen Second People's Hospital, The First Affiliated Hospital of Shenzhen University, Shenzhen, China
[2]International Cancer Center, Shenzhen University School of Medicine, Shenzhen, China
[3]Guangdong Key Laboratory of Systems Biology and Synthetic Biology for Urogenital Tumors, Shenzhen, China
[4]The First Affiliated Hospital of Shantou University, Shantou, China
[5]Shenzhen Institute of Synthetic Biology, Shenzhen Institutes of Advanced Technology, Chinese Academy of Sciences, Shenzhen, China

Correspondence

W Chen and W Huang, Shenzhen Second People's Hospital, The First Affiliated Hospital of Shenzhen University, Shenzhen 518035, Guangdong, China.
E-mails: jessie_chenwei@163.com (WC); hwrpony@email.szu.edu.cn (WH)

†Equal contributors.

Abstract

Objectives. Recent advances in patient-derived cancer organoids have opened a new avenue for personalised medicine. We aimed to establish an *in vitro* technological platform to evaluate chimeric antigen receptor (CAR)-T cell-mediated cytotoxicity against bladder cancer. **Methods.** Patient-derived bladder cancer organoids (BCOs) were derived using classic medium containing R-spondin 1 and noggin. The features of BCOs were characterised via H&E, whole-exome sequencing and immunofluorescence of specific markers. Surface antigen expression profiles of the recently identified CAR-recognisable targets were determined with a panel of antibodies via immunohistochemistry. A co-cultivation system consisting of BCOs and engineered T cells targeting a specific antigen was utilised to test its efficacy to model immunotherapy by cytotoxic assays and ELISA. **Results.** Bladder cancer organoid lines of basal and luminal subtypes were established. The histopathological morphology, genomic alteration, and specific marker expression profiles showed that the BCO lines retained the characteristics of the original tumors. Among all tested CAR-recognisable antigens in other solid tumors, MUC1 was simultaneously expressed in organoids and parental tumor tissues. Given the surface antigen profiles, second-generation CAR-T cells targeting MUC1 were prepared for modelling *in vitro* immunotherapy responses in BCOs. Specific immune cytotoxicity occurred only in the MUC1$^+$ organoids but not in the MUC1$^-$ organoids or control CAR-T cells. **Conclusion.** Patient-derived BCOs recapitulate the heterogeneity and key features of parental cancer tissues, and these BCOs could be useful for preclinical testing of CAR-T cells *in vitro*.

Keywords: bladder cancer, CAR-T, cytotoxicity evaluation, MUC1, organoid

INTRODUCTION

Bladder cancer is the ninth most prevalent cancer globally, with approximately 430 000 new cases diagnosed each year.[1] Clinically, approximately 75% of patients present with non-muscle-invasive bladder cancer (NMIBC), and the rest with muscle-invasive bladder cancer (MIBC).[2] This pathological classification and the characteristics of each subtype determine clinical management of this malignancy. Patients with NMIBC are usually treated with transurethral resection, followed by intravesical therapy. However, approximately 60% of patients relapse within 2 years after therapy, and 25% of these cases progress to advanced stages.[3] Currently, radical cystectomy and platinum-based chemotherapy are the therapeutic options available for MIBC. However, a large number of patients with MIBC develop metastatic spread, which is associated with extremely low survival rates.[4] Novel approaches such as immunotherapy are currently being investigated.

Recently, various immunotherapeutic approaches, namely, bacillus Calmette–Guérin (BCG) intravesical instillation and immune checkpoint blockade therapy have achieved durable clinical benefits in patients with bladder cancers of both early and advanced stage bladder cancers. In this regard, bladder cancer provides an appropriate experimental tumor model to inspect immunotherapy response, which could be translated into therapeutic approach for other solid cancers.[5,6] Additionally, owing to the heterogeneity and genetic instability of bladder cancer, personalised immunotherapy for individual patient represents an unmet challenge. Chimeric antigen receptor (CAR)-T cell is a promising personalised immunotherapeutic tool for solid cancers, as they can be modified to express a CAR for any tumor-associated antigen (TAA).[7] Although multiple early-phase CAR-T cell clinical trials for bladder cancer have been registered, no results have been published, including laboratory research results.[8] At this stage, developing a personalised CAR-T cell immunotherapy against bladder cancer is imperative.

In fact, any personalised immunotherapeutic strategy aiming to achieve clinical success has to be evaluated and verified via a large number of preclinical experiments. Traditional monolayer cultures of cell lines and animal models of patient-derived xenografts (PDXs) are the currently common options for preclinical evaluation.[9] Monolayer cell lines can be easily expanded *in vitro* with a simple technique, but are barely conducive for evaluation of therapeutic effect due to the lack of tumor characteristics.[10] PDXs allow for *in vivo* screening; however, it involves intensive time and resource.[11,12] The development of patient-derived organoids (PDOs) has solved the above problems well. A study has reported the development of a biobank of patient-derived bladder tumor organoids using hepatocyte media containing foetal bovine serum (FBS), and verified its application for clonal evolution and drug screening.[13] Another group successfully applied bladder cancer organoids for genetic modification and drug testing.[14]

In this study, a modified medium was used to culture BCOs from luminal and basal MIBC samples. Additionally, among the CAR-targetable antigens identified in other solid tumors, MUC1 was simultaneously expressed in organoids and the corresponding tumor tissues. A second-generation CAR that targets MUC1 was prepared, and we investigated the response of MUC1-expressing BCOs to CAR-T cells targeting MUC1. Therefore, a clear workflow for patient-derived BCOs cultivation and co-culture with CAR-T cells to determine the *in vitro* immune response was developed. This strategy will accelerate the translational research to improve personalised immunotherapy for bladder cancer and other solid tumors.

RESULTS

Bladder cancer organoids recapitulate the histological features of parental tumors

Components of the medium were optimised from previous prostate cancer organoid cultivation,[15] and we established three lines of BCOs that were derived from cystectomy specimens. Detailed clinic pathological data of patients and *in vitro* passage information of BCOs are summarised in Supplementary table 1. The initial BCOs were visible within 3–4 days after plating and displayed a solid spherical structure with a size of 20–300 μm. Those BCOs were passaged for more than 4 months without showing any decline in growth rate. Histological examination using haematoxylin & eosin (H&E) staining showed that the BCOs

displayed cancer-like morphology with nuclear and cellular atypia, a similar morphology to that of the epithelial components in their original tumor tissues (Figure 1). Interestingly, the bright-field image of BC03 revealed lumen-containing spheres of clear cells with a central lumen (Figure 1).

To further characterise the BCOs, we performed immunofluorescence analyses of marker expression in each organoid line, as well as their corresponding parental tumors. The results showed that the marker expression profiles were consistent between tumor tissues and their derived organoids. All the BCOs and their parental tumors expressed Ki67 and E-cadherin, confirming the epithelial origin and high proliferative activity of BCOs. Furthermore, based on the staining results of a series of markers, we could successfully categorise the tumor tissues and their derived BCOs into basal or luminal subtype. Although CK20 is not expressed in BC01, other luminal markers are positively stained in this sample. Furthermore, both BC01 and BC02 showed negative staining for any basal markers.
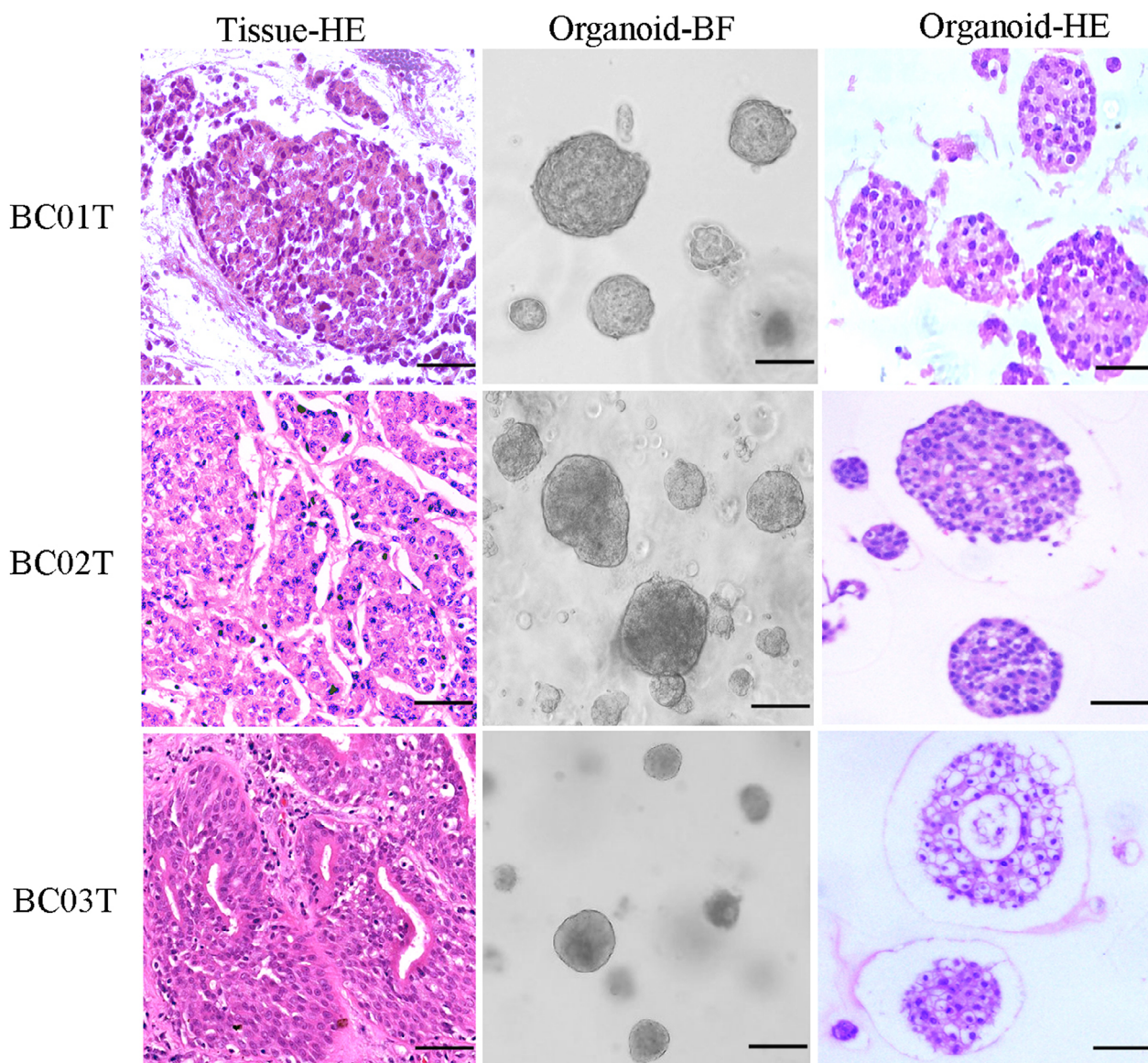

Figure 1. Patient-derived bladder cancer organoid cultures expand long-term *in vitro* while maintaining the histological architecture of their parental tumor. The middle column shows bright-field images of each organoid line, and the left and right panels show H&E staining of the organoids and their corresponding tissues, respectively. Scale bar, 100 μm.

Based on the negative staining for luminal markers (CK20, uroplakin II and GATA3) and positive staining for basal markers (CK5, P63 and CD44), BC03 was classified as basal subtype (Figure 2). To validate these findings, we performed RNA-sequencing (RNA-seq) analyses of parental tumors and organoid lines. Based on the gene signatures associated with basal and luminal defined from TCGA, a total of 486 differentiation genes were clearly divided into two clusters (basal
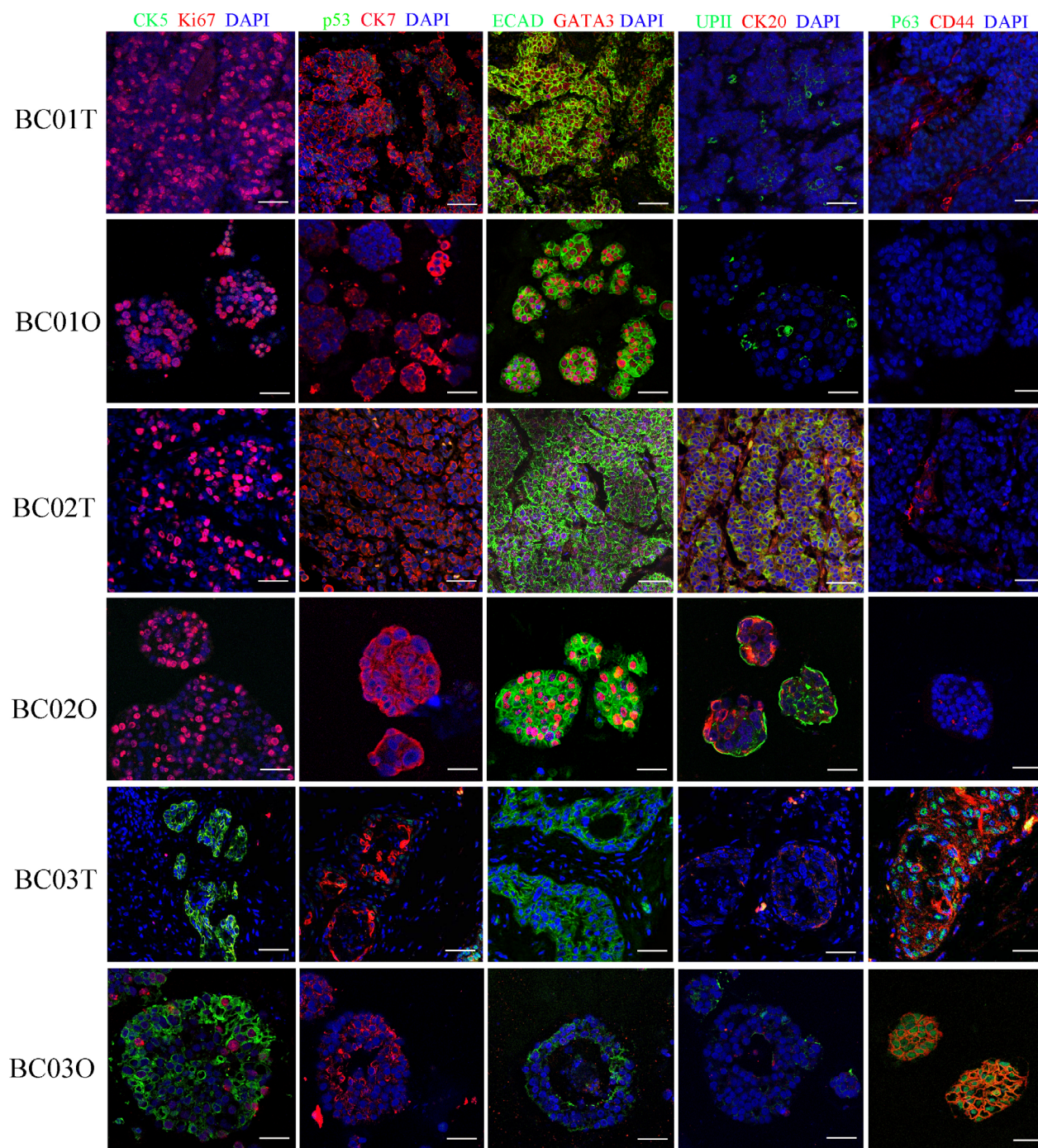

Figure 2. Immunofluorescence analysis of marker expression in parental tumors and patient-derived organoids. Tissues and organoids were stained for CK5, Ki67, p53, CK7, E-cadherin (ECAD), GATA3, uroplakin II (UPII), P63, CD44 and CK20 as indicated. Nuclei were counterstained with DAPI (blue). Scale bar, 100 μm.

or luminal). Although the stromal component of BC01O was lost during the culture, the gene expression profiles of BCOs were highly similar to that of their corresponding tissues. Molecular classification results based on RNA-seq data were consistent with the immunostaining results (Figure 3a).

Bladder cancer organoid lines retain the mutational spectrum of the parental tumors

To determine whether BCOs recapitulate the genomic profile of the primary tumors from which they were derived, we performed WES analysis of tumors and their derived BCOs. As expected, these tumors showed distinct somatic mutation profiles from each other. Notably, BCOs displayed a mutation profile that was highly compatible with their parental tumors. Several chromatin remodelling genes were enriched in the tumor and the organoids of BC01, including histone methyltransferase (e.g. *KMT2C*), histone acetylase (e.g. *CREBBP*) and a member of the SWI/SNF chromatin remodelling complex (e.g. *ARID1A*) (Figure 3b). Cell cycle regulator mutations were observed in the organoids and parental tumor of BC02. Co-mutation of *TP53* and *RB1* was observed in BC02, which indicates that its parental tumor was non-papillary bladder cancer[16] (Figure 3b). Further analysis of the proportion of exonic variations showed that both the single-nucleotide variants (SNVs) and indels in the original tissues were retained in the BCO lines. Additionally, the distribution of base substitutions in both tissues and organoids revealed a high proportion of the $C > T/G > A$ transition (Ti) and $C > A/G > T$ transversion (Tv), which is consistent with the mutational spectrum reported in MIBC[17] (Figure 3c). Copy number variations (CNV) affect a larger fraction of the genome in cancers than other types of somatic genetic alteration.[18] The results showed that multiple chromosomal aberrations consisting of gains and/or losses were highly conserved in the tissue-organoid pairs (Figure 3d).

High and consistent expression of the MUC1 in bladder cancer organoids and their original tumors

To obtain the specific surface antigen profiles of each tumor, a panel of antibodies against common targets of other solid tumors were tested in our samples via IHC. As shown in

Supplementary figure 1, MUC1 was the only antigen that was highly expressed among all tested antigens (B7-H3, vEGFR2, CEACAM5, HER2, FRα, GD2, EGFRvIII, PSMA, PSCA, MSLN, PD-L1 and CD44v6). Further immunofluorescence analysis showed consistent expression of MUC1 in corresponding BCOs but not in adjacent normal tissues (Figure 4). Therefore, MUC1 was used as a putative target to test the efficacy of specific CAR-T cells.

Construction of MUC1-specific CAR-T cells

Given the antigen expression profiles of the organoids, second-generation CAR-T cells targeting MUC1 were prepared, using the CAR consisting of the single-chain variable fragment (scFv) of a humanised anti-MUC1 monoclonal antibody (HMFG2), and the signalling domains from the costimulatory molecules CD28 and CD3ζ (Figure 5a). CAR-T cells targeting CD19 were used as a control. The expression of the CAR on T cells after lentivirus transduction was confirmed by detecting the co-expressed copGFP with fluorescence microscopy (Figure 5b), and flow cytometry (Figure 5c). The presence of the scFv sequence of anti-MUC1 in CAR-T cells was further confirmed by reverse transcription quantitative real-time polymerase chain reaction (RT-qPCR) (Figure 5d). The phenotype of CAR-T cells was also analysed by flow cytometry. Seven days after transduction, the ratio of $CD4^+:CD8^+$ T cells was approximately 1:3, and there was no significant difference between the CAR-T cells and CD19 CAR-T cells was observed (Figure 5e).

Quantitative analysis of CAR-mediated cytotoxicity in BCOs

To assess the utility of our BCOs for testing immunotherapeutic response in bladder cancer, we co-cultured $MUC1^+$ BCOs with MUC1-targeting CAR-T cells. Compared with CD19 CAR-T cells, the MUC1-targeting CAR-T cells spontaneously migrated towards the $MUC1^+$ BC01O and BC02O. Directional migration was not discernible when $MUC1^-$ organoids was co-cultured with MUC1 CAR-T cells (Figure 6a). Specifically, $MUC1^+$ organoids underwent deformation and cell lysis, and their surrounding CAR-T cells showed high expression of granzyme B (Figure 6b). The cytotoxic activity was analysed using a lactate dehydrogenase (LDH) release kit to further
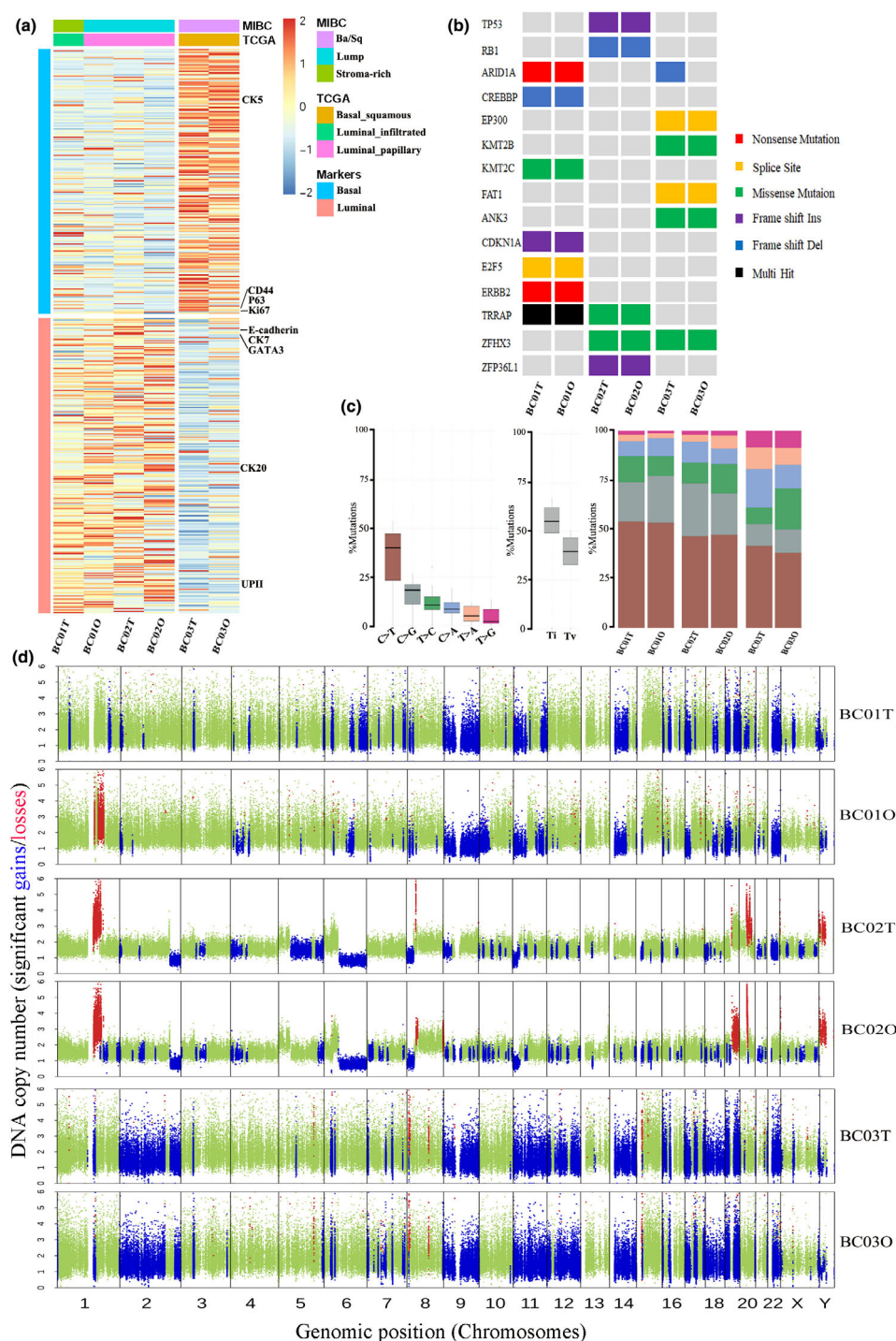
Figure 3. Repertoire of gene expression and genetic alterations found in the bladder cancer organoids and their original tumors. **(a)** Heatmaps showed the expression pattern of luminal and basal molecule profiles of tumors and corresponding organoid lines. The column annotation across the top provides the subtype calls from TCGA. Selected biomarkers used for immunostaining identification were labelled. **(b)** Overview of somatic mutations found in tissue-organoid pairs grouped by patient. Shown are those genes with the most mutations: examples include nonsense mutations (e.g. *ARID1A* and *ERBB2*), missense mutations, splice site mutations (e.g. *EP300* and *FAT1*), multiple hit mutations, and frame shift indels/dels (e.g. *TP53*, *RB1*, *CREBBP* and *CDKN1A*). **(c)** Percentage of the six types of SNVs, averaged across all samples. Proportions of exonic variants across the samples. The six types of SNVs are represented. **(d)** Scatterplots illustrating the genome-wide CNVs of the bladder cancer tissue-organoid pairs. The DNA copy number gains (blue) and losses (red) found in the original tissue were conserved in the derived organoid lines.
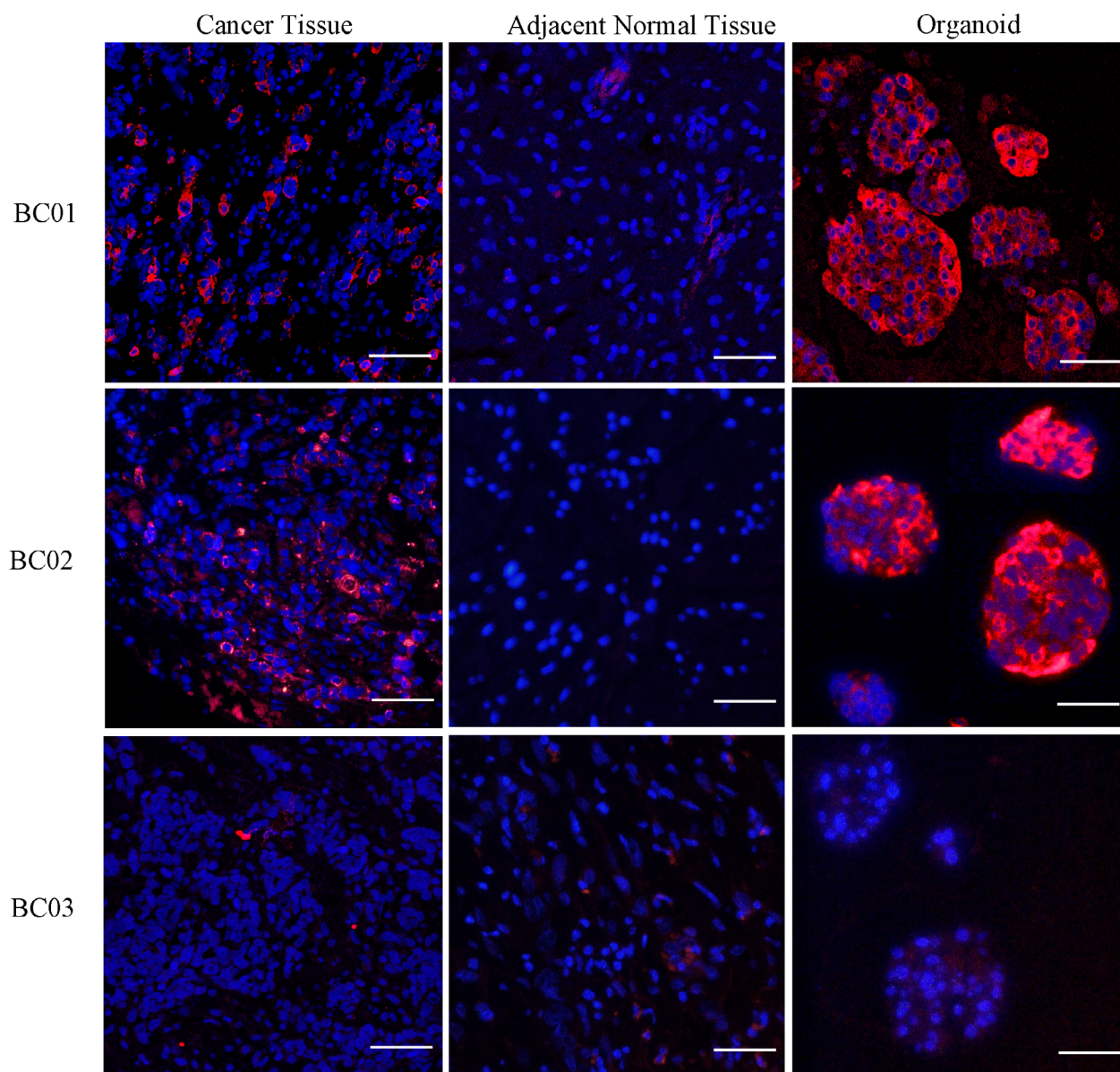
Figure 4. Expression of MUC1 in bladder cancer tissues, adjacent normal tissues and bladder cancer organoids. Nuclei were counterstained with DAPI (blue). Scale bar, 100 μm.

confirm the cell killing of MUC1 CAR-T cells. As shown in Figure 6c, LDH release was significantly higher in the MUC1 CAR-T cell group than in CD19-targeting CAR-T group and the MUC1$^-$ BCO group (***$P < 0.001$, Figure 6c). Additionally, the production of interleukin (IL)-2, interferon (IFN)-γ and tumor necrosis factor (TNF)-α was significantly increased only when MUC1 CAR-T cells were incubated with MUC1$^+$ BCOs. These results suggest specific antigen recognition and immune activation during co-culture (***$P < 0.001$, Figure 6c).

DISCUSSION

The availability of a readily accessible *in vitro* model which can faithfully recapitulate the original cancer tissue is of great importance for preclinical testing. Patient-derived cancer organoids are increasingly recognised as an optimal model for basic and translational research in solid tumors, considering their promising potential in the preclinical screening of personalised antitumor drugs.[19] Classic media containing R-spondin 1 (a Wnt agonist and ligand
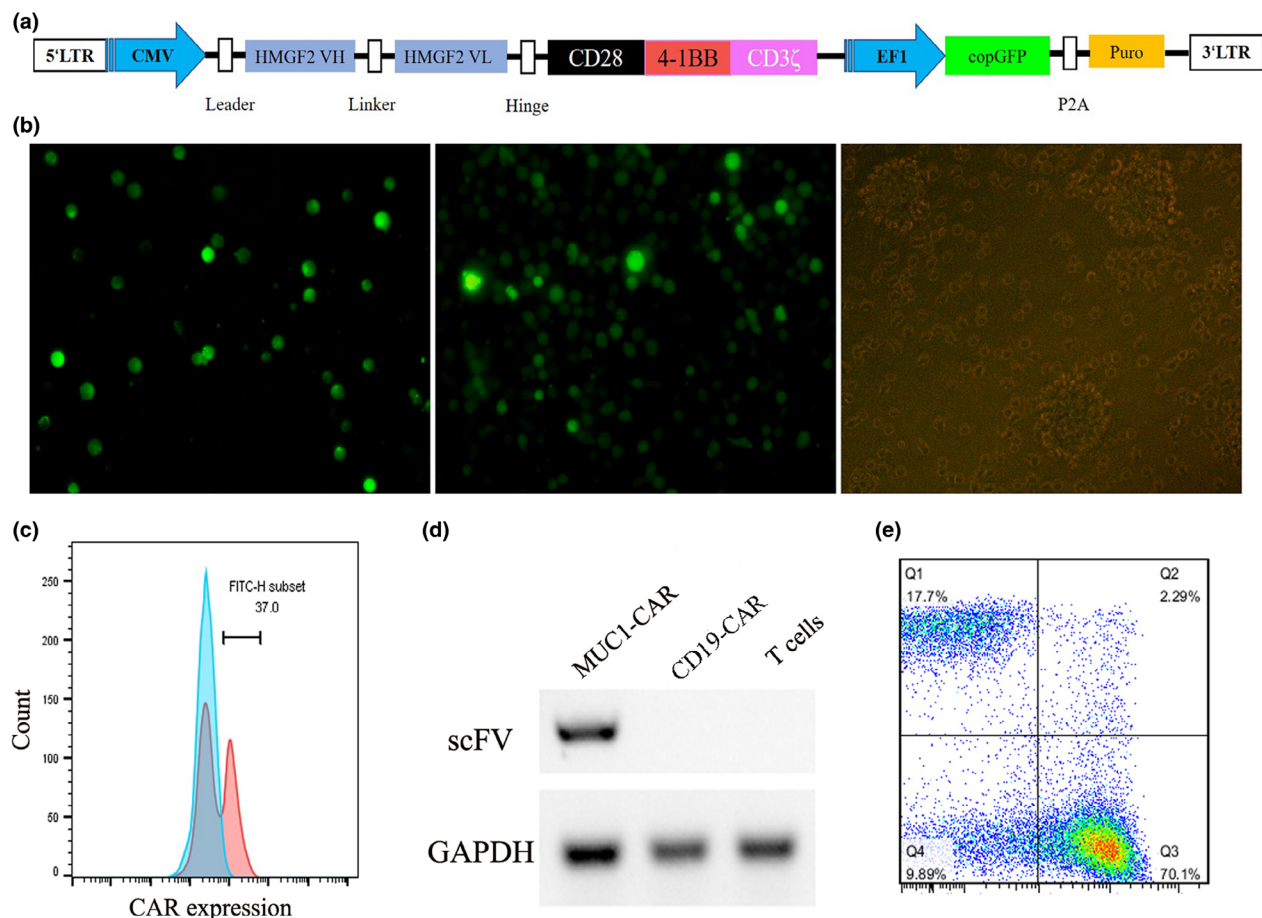
Figure 5. Construction of MUC1-specific CAR-T cells. **(a)** Schematic of the MUC1 CAR used in this study. **(b, c)** The transduction efficiency of the CAR was measured by the detection of copGFP using fluorescence microscopy **(b)** and flow cytometry analysis **(c)**. **(d)** Reverse transcription PCR detection MUC1 CAR-T cells, CD19 CAR-T cells and T cells. **(e)** CAR-T cell subtypes and phenotypes were analysed by flow cytometry 7 days after the transduction of the CAR lentivirus.

of LGR5), epidermal growth factor (EGF), and noggin (a bone morphogenetic protein inhibitor) were used to establish several types of tumor organoids, including organoids cultures of colorectal cancer,[20] prostate cancer,[21] pancreatic cancer,[22] breast cancer,[23] and liver cancer.[24] In this study, we made minor modifications to the medium recipe of prostate cancer organoids.[15] Specifically, we removed two prostate-specific factors (prostaglandin E2 and dihydrotestosterone), and increased the concentrations of EGF and fibroblast growth factor 2 to enable long-term expansion of BCO lines. These organoids faithfully recapitulated the morphological and genetic features of their parental tumors. Notably, of all the tested CAR-recognisable antigens common in other solid tumors, only MUC1 was consistently expressed in

the organoids and corresponding tumor tissues. Interestingly, one organoid line (BC03O) did not express MUC1, and was therefore used as a control for the subsequent testing of the immune response of BCOs.

The heterogeneity and genetic instability of bladder cancer indicate that cancer therapy, including CAR-T immunotherapy, should be personalised for each patient. Through screening with a panel of antibodies against recently identified targets in other solid tumors, we observed that MUC1 was the only surface antigen that was highly expressed in both the cancer tissues and their derived organoids. Interestingly, analysis of a large number of samples, including bladder cancer tissues ($n = 404$) and normal bladder tissues ($n = 28$) from The Cancer Genome Atlas (TCGA) database, showed that the expression of MUC1 in
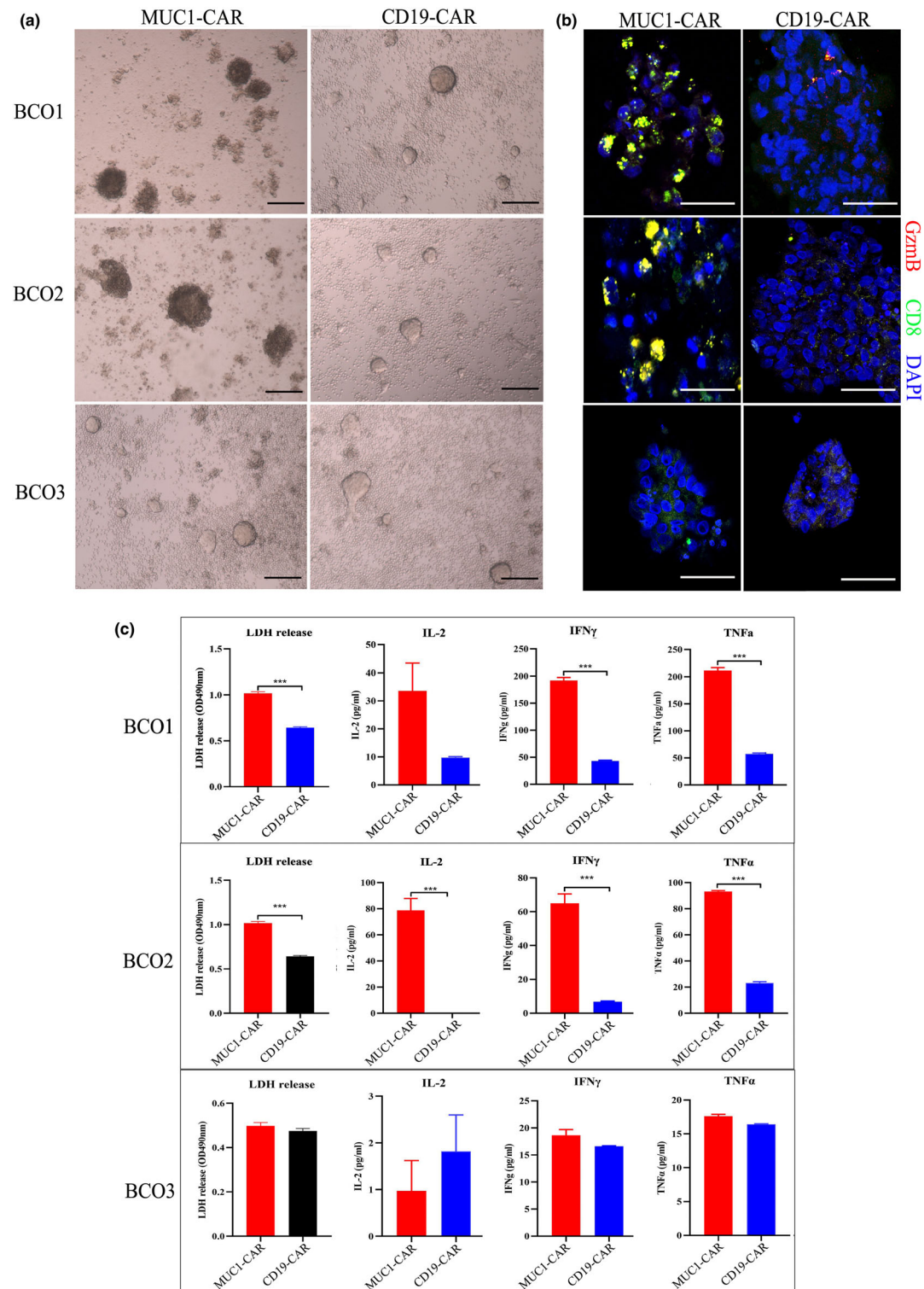
Figure 6. Modelling immunotherapy with co-culture of BCOs and CAR-T cells. **(a)** Images of the co-culture of BCOs with either MUC1 CAR-T cells or CD19 CAR-T cells at 72 h. Scale bar, 200 µm. **(b)** Immunostaining images of immunostaining for DAPI, CD8 and Granzyme B in BCOs after co-cultured with MUC1 CAR-T cells or CD19 CAR-T cells. Note the presence of activated and proliferation T cells near apoptotic BCOs. Scale bar, 100 µm. **(c)** Quantification of LDH release and cytokines products (IL-2, IFN-γ and TNF-α) from BCOs after co-culture with either MUC1 CAR-T cells or CD19 CAR-T cells. Values represent the mean ± SEM ($n = 3$; unpaired parametric t-test; ***$P < 0.001$).

cancer tissues was significantly higher than that in normal group (Supplementary figure 2). Additionally, other studies showed high serum level and high tissue expression of MUC1 in patients with advanced bladder cancer.[25,26] All the above evidence indicates that MUC1 can be used as a putative diagnostic and therapeutic marker for bladder cancer. Furthermore, the apical expression pattern with shorter glycans of MUC1 is characteristic of various malignancies, making MUC1 a highly attractive target for cancer immunotherapy.[27] Recently, CAR-T cells have been used to target MUC1-expressing cancers, such as non-small-cell lung carcinoma,[28] and pancreatic adenocarcinoma.[29] However, MUC1-targeted immunotherapy has not been reported for bladder cancer.

Recent reports indicate the potential application of a co-culture system containing patient-derived organoids (PDOs) and immune cells for assessing the efficacy of cancer immunotherapy and precision medicine.[30] In a previous study, the tumor immune microenvironment and the response to immune checkpoint blockade therapy were adequately modelled in the PDOs approach that preserves the original tumor T cell receptor spectrum.[31] Checkpoint inhibitors (CPIs) have been used as first-line treatment options for urothelial carcinoma metastatic patients with programmed death ligand 1 (PD-L1)-positive tumors and are platinum-ineligible.[32] However, IHC evaluation revealed extremely low expression of PD-L1 in our tissue samples and corresponding BCOs. Therefore, the potential role of BCOs for predicting the response to PD-L1 inhibitors or the combination of CPIs and CAR-T cells requires more organoid lines with high expression of PD-L1. Another group expanded the tumor-reactive T cells via continuous co-cultivation of peripheral blood lymphocytes with tumor organoids, and verified the anticancer properties of those tumor specific T cells.[33] Further research on the BCO-immune cell co-culture system is needed, and will be of great clinical interest to the medical community.

In summary, our patient-derived BCOs recapitulated the heterogeneity and key features of their parental bladder cancers. In this article, we present a clear workflow for personalised preclinical CAR-T cell testing in bladder cancers based on this PDOs model, and this will accelerate the translational research to improve personalised immunotherapy in bladder cancer and other solid tumors.

METHODS

Organoid culture

Surgically resected tissues were obtained from patients diagnosed with MIBC, and informed consent was obtained from all patients enrolled in this study. Each sample was divided into four parts: one randomly selected part was fixed in 10% neutral-buffered formalin for histopathological analysis, another randomly selected part was stored at $-80°C$ for sequencing, and the remaining portions were processed to derive organoids. The organoid derivation process included the following steps: bladder cancer tissues were minced and digested in 4 mL of 5 mg mL^{-1} collagenase type II (Invitrogen, Carlsbad, CA, USA) in the advanced Dulbecco's Modified Eagle Medium/Nutrient Mixture F-12 medium and digested for 45 min at 37°C. The remaining cell aggregates were further digested in 4 mL of TrypLE Express recombinant enzyme (Invitrogen) for another 5 min at 37°C. Subsequently, the suspension was then filtered through a 70-μm nylon cell strainer and centrifuged for 5 min at 300 g. The cell pellets were suspended in cold Matrigel, and Matrigel cell suspension were seeded in prewarmed 6-well culture plates. The drops were solidified for 1 min on the right side up and for another 9 min upside down at 37°C with 5% CO_2, after which 2 mL of organoid culture medium (Supplementary table 2) was added. For passaging, all drops were scraped, and the cells were digested with TrypLE Express with Y-27632 dihydrochloride (10 μM) for 5 min at 37°C. The cell pellets were resuspended in Matrigel and seeded as described previously.

Histological evaluation and immunofluorescence assay

Tissues were processed for paraffin sectioning using standard protocols. Organoid processing was performed in the following manner: organoids were scraped and fixed in 10% neutral-buffered formalin for at least 24 h. Cell pellets were collected by centrifugation and resuspended in melted 2% agarose. Solidified agarose drops were then dehydrated and embedded in paraffin, after which 4-μm paraffin sections were stained with H&E using standard protocols. For immunofluorescence tests, the slides were subjected to antigen retrieval using EDTA retrieval solution at pH 8.0. After rinsing with PBS, the slides were either stained with antibodies against bladder cancer markers or antibodies against common solid tumor surface antigens (Supplementary table 3). The appropriate fluorophore-conjugated secondary antibodies and 4′,6-diamidino-2-phenylindole (DAPI) (Supplementary table 4) were diluted 1:1000 and incubated for 1 h at room temperature. Images were obtained using a Zeiss LSM 880 confocal microscope (Zeiss, Oberkochen, Germany) and processed using the corresponding software.

Whole-exome sequencing and analysis

The genomic DNA of samples, including primary tissue, blood and organoids was isolated using the AllPrep DNA/RNA Mini

Kit. WES libraries were prepared according to the manufacturer's recommendations of the Agilent SureSelect Human All Exon V6 kit (Agilent Technologies, CA, USA). Paired-end sequencing (2 × 150 bp) was then performed using the Illumina Novaseq. The blood samples were sequenced to depths of 100 × (approximately 12 Gb/sample), and samples of tissues and organoids to the depths of 200 × (approximately 24 Gb/sample). Raw sequences were filtered by adaptor and low-quality reads using the Fastp software, v 0.12.6.[34] SNV calls were performed with the GATK toolkit, v3.6[35] based on comparison of the tumor or organoid with its corresponding blood sample. According to the best practice guidelines, sequence reads were mapped against the human reference genome (UCSC hg19) using the Burrows-Wheeler Aligner with Maximal Exact Matches (BWA-MEM) software, v0.7.12[36] followed by marked duplicates, merging of lanes, and realignment of indels. Somatic SNVs and indels were determined by subjecting the reference (blood) and tumor or organoid sequencing data to the Mutect2 and Strelka2 models,[37] respectively. Somatic SNVs with variant allele frequency < 0.05 and supported by fewer than three reads were filtered out. Copy number alternations (CNAs) were detected using the Control-FREEC software, v11.5[38] with BAM files. Mutation effect predictions and annotations were performed using the Annovar tool,[39] or the COSMIC and dbSNP databases.[40]

RNA sequencing and analysis

RNA was extracted from tumor samples and corresponding organoids. mRNA libraries were prepared using NEBNext®UltraTM RNA Library Prep Kit for Illumina® (NEB, USA) following the manufacturer's instructions. RNA sequencing was performed with PE 150 bp using Illumina Novaseq. After sequencing quality control, mapping and counting analysis were performed using STAR (v2.4.0j)[41] and RSEM.[42] Level-3 TCGA RNA-seq data of BLCA were downloaded from the TCGA Data Portal. Differential expression analysis between patients with basal and luminal phenotypes was performed using the Wilcoxon test. Genes with a P-value ≤ 0.01 and $|\log_2 FC| \geq 2.5$ were used as basal/luminal markers.

Chimeric antigen receptor T cell generation

The second-generation CAR structure was composed of the MUC1 mAb scFv (HMFG2) sequence linked to the IgD hinge, CD28 transmembrane region, and CD3ζ endodomain sequences.[27] These structures were synthesised and cloned into a lentivirus vector. Lentiviral particles were generated by co-transfection of the CAR vector with packaging plasmids using Lipo3000 (Invitrogen). The supernatant was collected at 48 and 72 h, and subsequently centrifuged at 50 000 g for 2 h at 4°C. The pellet was resuspended in cold PBS, aliquoted and stored at −80°C.

Whole peripheral blood obtained from healthy volunteers and peripheral blood mononuclear cells (PBMCs) were isolated by Ficoll density gradient centrifugation. CD3$^+$ T cells were magnetically sorted using CD3 beads. Purified T cells were further stimulated by incubation with CD3/CD28 beads for 2 days prior to use. T cells were cultured in RMPI 1640 (Gibco) supplemented with 10% FBS, 100 IU mL^{-1} of a penicillin–streptomycin mixture, 50 IU mL of IL-2 and 1 ng mL^{-1} of IL-15. Activated T cells were transduced with lentivirus (MOI = 50) with 8 μg mL^{-1} of polybrene in the presence of IL-2. T cells were cultured after the addition of 50 IU mL^{-1} of IL-2 and 1 ng mL^{-1} of IL-15 for 7–10 days before use.

Flow cytometry analysis

Cells for transduction efficiency analysis were filtered through a 35-μm nylon mesh and immediately analysed via the FITC channel. Cells for phenotype analysis were filtered through a 35-μm nylon mesh, washed twice with PBS containing 0.5% FBS, and subsequently incubated with a panel of antibodies against CD3 (APC), CD4 (PE) and CD8 (FITC) (BD Pharmingen, Franklin Lakes, NJ, USA) for 30 min in the dark at room temperature. All flow cytometric analyses of cells were performed using a FACSAria flow cytometer (BD), and data were analysed using the FlowJo software v8.8.7 (Treestar Inc, Ashland, OR, USA).

Reverse transcription PCR

Total RNA was isolated from T cells using the Blood RNA kit (Biomiga, San Diego, CA, USA) and reverse transcribed into cDNA using the ReverTra qPCR RT kit (TOYOBO, Osaka, Japan). The following primers were used for RT-qPCR: GAPDH-forward: 5′-GACCACAGTCCATGCCATCA-3′, GAPDH-reverse: 5′-CATCACGCCACAGTTTCCC-3′, scFv of CAR-MUC1-forward: 5′-GAGCAAAGACGGGACAGC-3′, scFv of CAR-MUC1-reverse: 5′-AGCCAGGACTCCACCAACC-3′.

Co-culture of bladder cancer organoids with chimeric antigen receptor T cells

Bladder cancer organoids were scraped and centrifuged at 300 g for 3 min, followed by digestion in 4 mL of TrypLE Express at 37°C for 3 min. Trypsinisation was discontinued by the addition of 6 mL of 20% FBS advanced media, followed by centrifugation at 300 g. The dissociated organoids were resuspended in organoid media and plated in the middle of a precoated 48-well plate containing 50% Matrigel. After being maintained in an incubator overnight, the organoid medium was discarded and replaced with 500 μL of X-VIVO™ 15, a serum-free haematopoietic cell medium (Lonza), which was also used to resuspend control T cells and CAR-engineered T cells.

Cytokine detection assays

We sampled 50 μL of the medium from each well after BCO-CAR-T cell co-culture. An enzyme-linked immunosorbent assay (ELISA) was performed in duplicate on a 2-fold-diluted medium using human IL-2, TNF-α and IFN-γ ELISA kits (BD) according to the manufacturer's instructions. The optical density was measured at 450 nm using the VICTOR Nivo system (Perkin Elmer, Waltham, MA, USA).

CONFLICT OF INTEREST

The authors declare no conflict of interest.

AUTHOR CONTRIBUTIONS

Lei Yu: Conceptualization; Data curation; Investigation; Methodology; Project administration; Writing-original draft. **Zhichao Li:** Data curation; Investigation; Methodology; Writing-review & editing. **Hongbin Mei:** Data curation; Funding acquisition; Resources. **Wujiao Li:** Data curation; Investigation. **Dong Chen:** Investigation; Methodology. **Lisa Liu:** Investigation; Methodology. **Zhongfu Zhang:** Data curation; Resources. **Yangyang Sun:** Methodology; Writing-review & editing. **Fei Song:** Funding acquisition; Methodology; Writing-review & editing. **Wei Chen:** Conceptualization; Methodology; Project administration; Writing-review & editing. **Weiren Huang:** Conceptualization; Funding acquisition; Project administration.

REFERENCES

1. Antoni S, Ferlay J, Soerjomataram I, Znaor A, Jemal A, Bray F. Bladder cancer incidence and mortality: a global overview and recent trends. *Eur Urol* 2017; **71**: 96–108.
2. Kamat AM, Hahn NM, Efstathiou JA *et al*. Bladder cancer. *Lancet* 2016; **388**: 2796–2810.
3. Chamie K, Litwin MS, Bassett JC *et al*. Recurrence of high-risk bladder cancer: a population-based analysis. *Cancer* 2013; **119**: 3219–3227.
4. Martinez VG, Munera-Maravilla E, Bernardini A *et al*. Epigenetics of bladder cancer: where biomarkers and therapeutic targets meet. *Front Genet* 2019; **10**: 1–24.
5. Song D, Powles T, Shi L, Zhang L, Ingersoll MA, Lu YJ. Bladder cancer, a unique model to understand cancer immunity and develop immunotherapy approaches. *J Pathol* 2019; **249**: 151–165.
6. Wolacewicz M, Hrynkiewicz R, Grywalska E *et al*. Immunotherapy in bladder cancer: current methods and future perspectives. *Cancers (Basel)* 2020; **12**: 1–17.
7. Koneru M, Purdon TJ, Spriggs D, Koneru S, Brentjens RJ. IL-12 secreting tumor-targeted chimeric antigen receptor T cells eradicate ovarian tumors *in vivo*. *Oncoimmunology* 2015; **4**: e994446.
8. Pantuck M, Palaskas N, Drakaki A. Next generation T-cell therapy for genitourinary malignancies, part A: Introduction and current state of the art. *Cancer Treat Res Commun* 2018; **17**: 8–12.
9. Jarno Drost HC. Organoids in cancer research. *Nat Rev* 2018; **18**: 407–418.
10. Horvath P, Aulner N, Bickle M *et al*. Screening out irrelevant cell-based models of disease. *Nat Rev Drug Discov* 2016; **15**: 751–769.
11. Ben-David U, Ha G, Tseng YY *et al*. Patient-derived xenografts undergo mouse-specific tumor evolution. *Nat Genet* 2017; **49**: 1567–1575.
12. Byrne AT, Alferez DG, Amant F *et al*. Interrogating open issues in cancer medicine with patient-derived xenografts. *Nat Rev Cancer* 2017; **17**: 254–268.
13. Lee SH, Hu W, Matulay JT *et al*. Tumor evolution and drug response in patient-derived organoid models of bladder cancer. *Cell* 2018; **173**: 515–528.
14. Mullenders J, de Jongh E, Brousali A *et al*. Mouse and human urothelial cancer organoids: a tool for bladder cancer research. *Proc Natl Acad Sci USA* 2019; **116**: 4567–4574.
15. Drost J, Karthaus WR, Gao D *et al*. Organoid culture systems for prostate epithelial and cancer tissue. *Nat Protoc* 2016; **11**: 347–358.
16. Dinney CP, McConkey DJ, Millikan RE *et al*. Focus on bladder cancer. *Cancer Cell* 2004; **6**: 111–116.
17. Robertson AG, Kim J, Al-Ahmadie H *et al*. Comprehensive molecular characterization of muscle-invasive bladder cancer. *Cell* 2018; **171**: 540–556.
18. Zack TI, Schumacher SE, Carter SL *et al*. Pan-cancer patterns of somatic copy number alteration. *Nat Genet* 2013; **45**: 1134–1140.
19. Kondo J, Inoue M. Application of cancer organoid model for drug screening and personalized therapy. *Cells* 2019; **8**: 1–16.
20. van de Wetering M, Francies HE, Francis JM *et al*. Prospective derivation of a living organoid biobank of colorectal cancer patients. *Cell* 2015; **161**: 933–945.
21. Gao D, Vela I, Sboner A *et al*. Organoid cultures derived from patients with advanced prostate cancer. *Cell* 2014; **159**: 176–187.
22. Boj SF, Hwang CI, Baker LA *et al*. Organoid models of human and mouse ductal pancreatic cancer. *Cell* 2015; **160**: 324–338.
23. Sachs N, de Ligt J, Kopper O *et al*. A living biobank of breast cancer organoids captures disease heterogeneity. *Cell* 2018; **172**: 373–386.
24. Broutier L, Mastrogiovanni G, Verstegen MMA *et al*. Human primary liver cancer–derived organoid cultures for disease modeling and drug screening. *Nat Med* 2017; **23**: 1424–1435.
25. Simms MS, Hughes OD, Limb M, Price MR, Bishop MC. MUC1 mucin as a tumour marker in bladder cancer. *BJU Int* 1999; **84**: 350–352.
26. Kaur S, Momi N, Chakraborty S *et al*. Altered expression of transmembrane mucins, MUC1 and MUC4, in bladder cancer: pathological implications in diagnosis. *PLoS One* 2014; **9**: e92742.
27. Wilkie S, Picco G, Foster J *et al*. Retargeting of human T cells to tumor-associated MUC1: the evolution of a chimeric antigen receptor. *J Immunol* 2008; **180**: 4901–4909.

28. Wei XR, Lai YX, Li J *et al*. PSCA and MUC1 in non-small-cell lung cancer as targets of chimeric antigen receptor T cells. *Oncoimmunology* 2017; **6**: e1284722.

29. Posey AD Jr, Schwab RD, Boesteanu AC *et al*. Engineered CAR T cells targeting the cancer-associated Tn-Glycoform of the membrane mucin MUC1 control adenocarcinoma. *Immunity* 2016; **44**: 1444–1454.

30. Homicsko K. Organoid technology and applications in cancer immunotherapy and precision medicine. *Curr Opin Biotechnol* 2020; **65**: 242–247.

31. Neal JT, Li X, Zhu J *et al*. Organoid modeling of the tumor immune microenvironment. *Cell* 2018; **175**: 1972–1988.

32. Nadal R, Bellmunt J. Management of metastatic bladder cancer. *Cancer Treat Rev* 2019; **76**: 10–21.

33. Dijkstra KK, Cattaneo CM, Weeber F *et al*. Generation of tumor-reactive T cells by co-culture of peripheral blood lymphocytes and tumor organoids. *Cell* 2018; **174**: 1586–1598.

34. Chen S, Zhou Y, Chen Y, Gu J. fastp: an ultra-fast all-in-one FASTQ preprocessor. *Bioinformatics* 2018; **34**: 884–890.

35. McKenna A, Hanna M, Banks E *et al*. The genome analysis toolkit: a MapReduce framework for analyzing next-generation DNA sequencing data. *Genome Res* 2010; **20**: 1297–1303.

36. Li H, Durbin R. Fast and accurate short read alignment with Burrows-Wheeler transform. *Bioinformatics* 2009; **25**: 1754–1760.

37. Kim S, Scheffler K, Halpern AL *et al*. Strelka2: fast and accurate calling of germline and somatic variants. *Nat Methods* 2018; **15**: 591–594.

38. Boeva V, Popova T, Bleakley K *et al*. Control-FREEC: a tool for assessing copy number and allelic content using next-generation sequencing data. *Bioinformatics* 2012; **28**: 423–425.

39. Wang K, Li M, Hakonarson H. ANNOVAR: functional annotation of genetic variants from high-throughput sequencing data. *Nucleic Acids Res* 2010; **38**: 1–7.

40. Sherry ST, Ward MH, Kholodov M *et al*. dbSNP: the NCBI database of genetic variation. *Nucleic Acids Res* 2001; **29**: 308–311.

41. Dobin A, Davis CA, Schlesinger F *et al*. STAR: ultrafast universal RNA-seq aligner. *Bioinformatics* 2013; **29**: 15–21.

42. Li B, Dewey CN. RSEM: accurate transcript quantification from RNA-Seq data with or without a reference genome. *BMC Bioinformatics* 2011; **12**: 1–16.

Supporting Information

Additional supporting information may be found online in the Supporting Information section at the end of the article.